Heat Transfer to Magnetohydrodynamic Non-Newtonian Couple Stress Pulsatile Flow Between two Parallel Porous Plates

Samuel Olumide Adesanya[a] and Oluwole Daniel Makinde[b]

[a] Department of Mathematical Sciences, Redeemer's University, Redemption City, Nigeria
[b] Institute for Advance Research in Mathematical Modelling and Computations, Cape Peninsula University of Technology, P.O. Box 1906, Bellville 7535, South Africa

Reprint requests to S. O. A.; E-mail: adesanyaolumide@yahoo.com

Z. Naturforsch. **67a,** 647 – 656 (2012) / DOI: 10.5560/ZNA.2012-0073
Received March 1, 2012 / revised June 27, 2012 / published online October 10, 2012

This paper investigates the effect of radiative heat transfer to oscillatory hydromagnetic non-Newtonian couple stress fluid flow through a porous channel with non-uniform wall temperature due to periodic heat input at the heated wall. Based on some simplifying assumptions, the dimensionless partial differential equations are transformed into a set of ordinary differential equations and then solved using the Adomian decomposition method. The effects of the flow parameters on temperature and velocity profiles are shown graphically and discussed

Key words: Heat Transfer; Erying–Powel Model; Couple Stresses; Thermal Radiation.
Mathematics Subject Classification 2000: 76B, 76DXX

1. Introduction

Fluids that exhibit oscillatory flow have many important applications in nature, common examples in medical sciences included; blood flow through an artery, peristaltic food motion in the intestine, motion of urine in urethra to mention just a few. In recent times, there have been several important studies gearing towards this direction. For instance, the effect of couple stresses on an unsteady magnetohydrodynamic (MHD) non-Newtonian flow between two parallel fixed porous plates under a uniform external magnetic field using the Eyring–Powel model was studied in [1]. They reported that the flow is damped with increasing effect of couple stresses. In a related study, Zueco and Bég [2] presented the network simulation method (NSM) solution to a mathematical model for the laminar, pulsatile, non-Newtonian flow in a biofluid (blood) in a two-dimensional porous walled channel using the Eyring–Powell power law model incorporating polar couple stress effects. Their results showed that increasing non-Newtonian viscosity and couple stress effects decelerate the flow while increase in both steady and pulsating pressure gradient components accelerates the flow through the channel. Recently, Adesanya and Ayeni [3] examined the unsteady flow of an incompressible hydromagnetic, non-Newtonian fluid flow using the Eyring–Powell power law model and incorporating the polar couple stress effects through a porous channel. It was assumed that the channel is filled with a saturated porous medium and the fluid has variable viscosity. In the work, it was shown that the problem has a solution and the solution is unique.

All the above studies are limited to the hydrodynamic case in which the effects of heat transfer to the fluid flow are neglected. However, in many engineering and industrial processes like metallurgical engineering and polymer melts, flow occurs at a very high temperature. Therefore, the effect of radiation becomes significant for the final product to cool to room temperature. In recent times, there have been many studies on the radiative heat transfer to oscillatory flows, and different mathematical descriptions of these flows have been developed by several authors. These include the effects of free convection currents on the oscillatory flow of a viscoelastic fluid with thermal relaxation in the presence of a transverse magnetic field, which was bounded by a vertical plane surface studied in [4]. It was discovered that the velocity decreased in both cases of cooling and heating of the surface when compared to the Newtonian case. Also Makinde and Mhone [5] investigated the combined effects of radia-

tive heat transfer and magnetohydrodynamics on an oscillatory flow in a channel filled with a porous medium by using an analytical approach. They reported that increasing the magnetic field intensity reduces the wall shear stress while increasing the radiation parameter through heat absorption causes an increase in the magnitude of wall shear stress. Moreover, in [6] the unsteady oscillatory flow of an incompressible viscous fluid in a planar channel filled with a porous medium in the presence of a transverse magnetic field has been investigated. They observed that fluid slip at the lower wall increases the velocity at the wall and also that the Hartmann number, the porosity parameter, and the Grashof number weakens the slip at the wall while the Peclet number strengthens the slip. Furthermore, Hakeem and Sathiyanathan [7] presented analytical solutions for a two-dimensional oscillatory flow on free convective radiation of an incompressible viscous fluid through a highly porous medium bounded by an infinite vertical plate. They discovered that both velocity and temperature profiles accelerate with an increase in the radiation parameter. While in [8], a meshless numerical approach to study oscillatory Stokes flows in convection and convective flows in porous media by using the method of fundamental solutions was developed. The numerical results obtained showed an excellent agreement when compared with the analytical solutions of the problem. It was shown that the temperature is higher near the plate with injection while the velocity is enhanced near the plate with suction in a suction/injection controlled free convective motion of a viscous incompressible fluid between two periodically heated infinite vertical parallel plates [9].

Studies on non-Newtonian fluids have received much attention in recent years due to the inability of the Newtonian model to predict the rheological behaviour of complex fluids. Over the years, there have been many models to study the behaviour of many non-Newtonian fluids. One of these models is the couple stress fluid that is based on the Stokes microcontinuum theory in which the particle-size effects have been taken into consideration. These fluids are useful as fluid film in some engineering applications like rotor bearings [10, 11] and blood flow [12, 13]. Other notable research works on heat transfer to oscillatory fluid flow are [14, 15]. More recently, an analysis to investigate the Hall and ion-slip effects on fully developed electrically conducting couple stress fluid flow between vertical parallel plates in the presence of a temperature dependent heat source was conducted. In all the studies above the effect of radiative heat transfer to oscillatory hydromagnetic non-Newtonian optically thin couple stress fluid flow through a porous channel with non-uniform wall temperature due to periodic heat input at the heated wall has not been investigated.

Therefore, the main objective of this paper is to investigate the effect of radiative heat transfer on hydromagnetic non-Newtonian couple stress fluid flow through porous parallel plates with non-uniform wall temperature using the Erying–Powel model, which has not been accounted for in previous mathematical models. To achieve this, a computational approach based on the Adomian decomposition method (ADM) introduced by Adomian [16] is used to analyse the mathematical model. The method has been applied to different mathematical problems some of which are fractional-order differential equations [17], time dependent Edem–Fowler type equation [18], Navier–Stokes equations [19], evolution model [20], Flierl–Petviashivili equation [21], fourth-order wave equation [22], peristaltic transport model [23], Fokker–Planck equation [24], and extended Orr–Summerfield equation [25].

The rest of the paper is arranged as follows: Section 2 presents the formulation of the problem while in Section 3 analytical solutions of the problem are obtained, and results are discussed in Section 4. In Section 5, we give some concluding remarks.

2. Mathematical Formulation

Consider the unsteady mixed convection with thermal radiation of a viscous, incompressible, and electrically conducting flow through a porous channel. The fluid is assumed an optically thin couple stress non-Newtonian fluid under the influence of an externally applied homogeneous magnetic field and radiative heat transfer. The fluid is injected into the cold wall at $y = 0$ and sucked through the heated wall at $y = L$ with a uniform velocity v_0. All fluid properties are assumed constant except for fluid density that varies with temperature. We further assume that the fluid has small electrical conductivity, and the electromagnetic force produced is very small. Take a Cartesian coordinate system (x, y) where the x-axis lies along the centre of the channel; y is the distance measured in the normal section, see Figure 1.

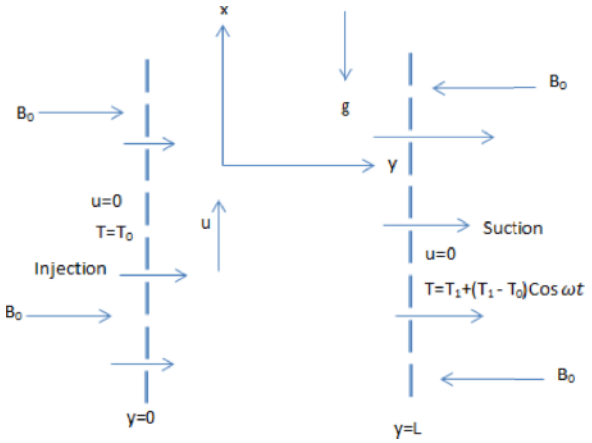

Fig. 1 (colour online). Geometry of the problem.

Assuming a Boussinesq incompressible fluid model, where the equations governing the fluid motion are given as

$$\rho\left(\frac{\partial u'}{\partial t'}+v_0\frac{\partial u'}{\partial y'}\right)=-\frac{\partial p'}{\partial x'}+\frac{\partial}{\partial y'}\tau_{xy} - \sigma_e B_0^2 u'-\eta\frac{\partial^4 u'}{\partial y'^4}+\rho g\beta\left(T'-T_0\right), \tag{1}$$

$$\rho C_p\left(\frac{\partial T'}{\partial t'}+v_0\frac{\partial T'}{\partial y'}\right)=k\frac{\partial^2 T'}{\partial y'^2}-\frac{\partial q_r}{\partial y'}, \tag{2}$$

where u', t', T', and p' are the axial velocity, the time, the fluid temperature, and the pressure. ρ is the fluid density, v_0 the suction/injection parameter, τ_{xy} the stress tensor, σ_e the conductivity of the fluid, B_0 the electromagnetic induction, η the couple stress parameter, g the gravitational force, β the coefficient of volume expansion due to temperature, C_p the specific heat at constant pressure, k the thermal conductivity, and q_r the radiative heat flux. It is

$$u'=0,\ u'_{yy}=0,\ T'=T_0 \ \text{ on } \ y=0, \tag{3}$$

$$u'=0,\ u'_{yy}=0,\ T'=T_1+(T_1-T_0)\cos\omega t \ \text{ on } \ y=h. \tag{4}$$

We assume that the fluid does not absorb its own radiations but absorbs radiations from the boundaries hence the radiative heat flux in the energy equation has been approximated in the optically thin limit. For a heat emitting fluid, the radiative heat flux for an optically thin fluid takes the form

$$\frac{\partial q_r}{\partial y'}=4I_2(T'-T_0), \tag{5}$$

where I_2 is the mean radiation parameter. The stress tensor in the Eyring–Powell model for non-Newtonian fluids is given by

$$\tau_{xy}=\mu\frac{\partial u'}{\partial y'}+\frac{1}{\alpha}\sinh^{-1}\left(\frac{1}{c}\frac{\partial u'}{\partial y'}\right), \tag{6}$$

where α, c are characteristics of the Erying–Powell model, and μ is the fluid dynamic viscousity. Linearizing the elastic part (6), since a higher-order expansion is negligible, we get

$$\sinh^{-1}\left(\frac{1}{c}\frac{\partial u'}{\partial y'}\right)\cong\frac{1}{c}\frac{\partial u'}{\partial y'}+O(\ )^3;\ \left|\frac{1}{c}\frac{\partial u'}{\partial y'}\right|<1, \tag{7}$$

Now we introduce the dimensionless parameters and variables as

$$\begin{aligned} &u=\frac{u'}{v_0},\ x=\frac{x'}{L},\ y=\frac{y'}{L},\ t=\frac{v_0 t'}{L},\\ &p=\frac{p'}{\rho v_0^2},\ H^2=\frac{\sigma B_0^2 L^2}{\mu},\ M=\frac{1}{\alpha c\mu},\\ &a^2=\frac{L^2\mu}{\eta},\ N^*=1+M,\ \theta=\frac{T-T_0}{T_w-T_0},\\ &\mathrm{Pe}=\frac{v_0 L\rho C_p}{k},\ \delta=\frac{4I_2}{v_0\rho C_p},\\ &\mathrm{Gr}=\frac{g\beta(T_w-T_0)}{\nu v_0},\ \mathrm{Re}=\frac{v_0 L}{\nu}, \end{aligned} \tag{8}$$

where H^2, M, a^2, Pe, Gr, and Re, are the Hartmann number, the Eyring–Powel parameter, the inverse of the couple stress parameter, the Peclet number, the Grashof number, and the Reynolds number. L is the channel characteristic length, θ the dimensionless temperature, and δ the thermal radiation parameter.

Using (5)–(8) in (1)–(4), we obtain the dimensionless equations

$$\frac{\partial u}{\partial t}+\frac{\partial u}{\partial y}=-\frac{\mathrm{d}p}{\mathrm{d}x}+\frac{N^*}{\mathrm{Re}}\frac{\partial^2 u}{\partial y^2}-\frac{H^2 u}{\mathrm{Re}} -\frac{1}{a^2\mathrm{Re}}\frac{\partial^4 u}{\partial y^4}+\mathrm{Gr}\theta, \tag{9}$$

$$\frac{\partial\theta}{\partial t}+\frac{\partial\theta}{\partial y}=\frac{1}{\mathrm{Pe}}\frac{\partial^2\theta}{\partial y^2}-\delta\theta. \tag{10}$$

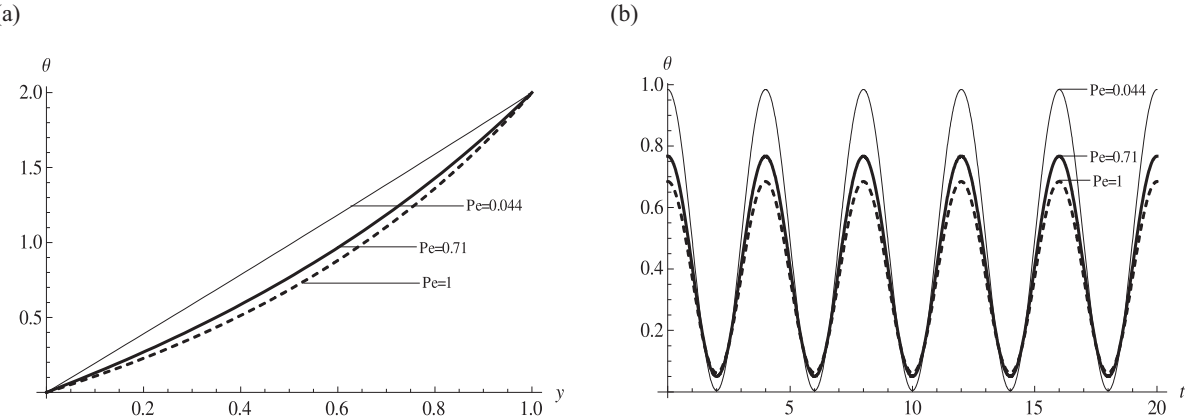

Fig. 2. (a) Effect of Peclet number on the temperature distribution plotted against position; (b) effect of Peclet number on the temperature distribution plotted against time.

Together with appropriate boundary conditions

$$u=0,\ \ u_{yy}=0,\ \ \theta=0\ \ \text{on}\ \ y=0, \tag{11}$$

$$u=0,\ \ u_{yy}=0,\quad \theta=1+\cos\omega t\ \ \text{on}\ \ y=1. \tag{12}$$

3. Method of Solution

The boundary conditions (11)–(12) suggest that the perturbative expressions

$$-\frac{\mathrm{d}p}{\mathrm{d}x}=p_1+p_0\,\mathrm{e}^{\mathrm{i}\omega t}, \tag{13}$$

$$u=v(y)+w(y)\,\mathrm{e}^{\mathrm{i}\omega t}, \tag{14}$$

$$\theta=A(y)+B(y)\,\mathrm{e}^{\mathrm{i}\omega t} \tag{15}$$

can be used to resolve the temperature and velocity field into a steady and periodic part. Where p_1,p_0 are positive constants, and ω is the frequency of oscillation for $t\geq 0$. Substituting (13)–(15) in (9)–(12) and equating the periodic and non-periodic terms, we obtain the following set of ordinary differential equations:

$$A''(y)-\mathrm{Pe}A'(y)-\mathrm{Pe}\delta A(y)=0, \tag{16}$$

$$B''(y)-\mathrm{Pe}B'(y)-\mathrm{Pe}(\delta+\mathrm{i}\omega)B(y)=0, \tag{17}$$

$$\frac{\mathrm{d}^4v}{\mathrm{d}y^4}=a^2\left(\mathrm{Re}p_1+\mathrm{Gr}A(y)-\mathrm{Re}\frac{\mathrm{d}v}{\mathrm{d}y}+\beta\frac{\mathrm{d}^2v}{\mathrm{d}y^2}-H^2v\right), \tag{18}$$

$$\frac{\mathrm{d}^4w}{\mathrm{d}y^4}=a^2\left(\mathrm{Re}P_0+\mathrm{Gr}B(y)-\mathrm{Re}\frac{\mathrm{d}w}{\mathrm{d}y}+\beta\frac{\mathrm{d}^2w}{\mathrm{d}y^2}-(H^2+\mathrm{iRe}\omega)w\right), \tag{19}$$

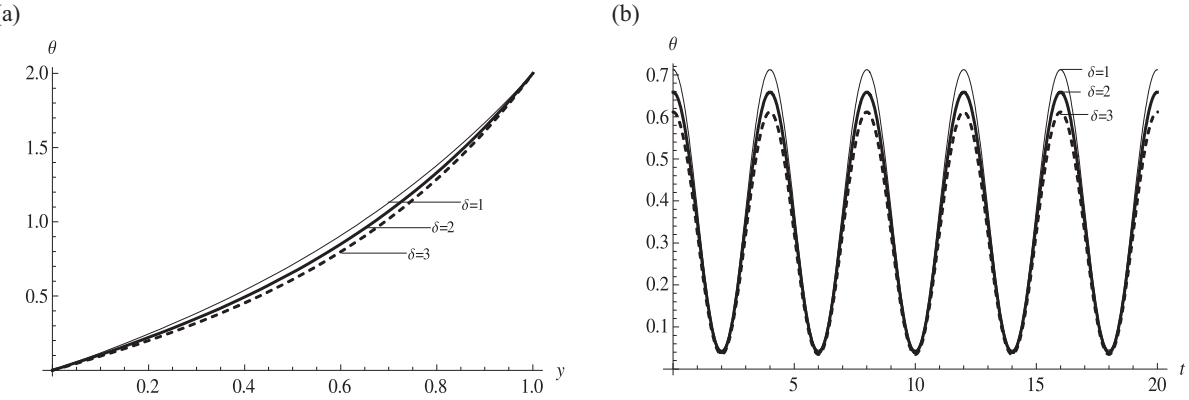

Fig. 3. (a) Temperature distribution plotted against position; (b) temperature distribution plotted against time.

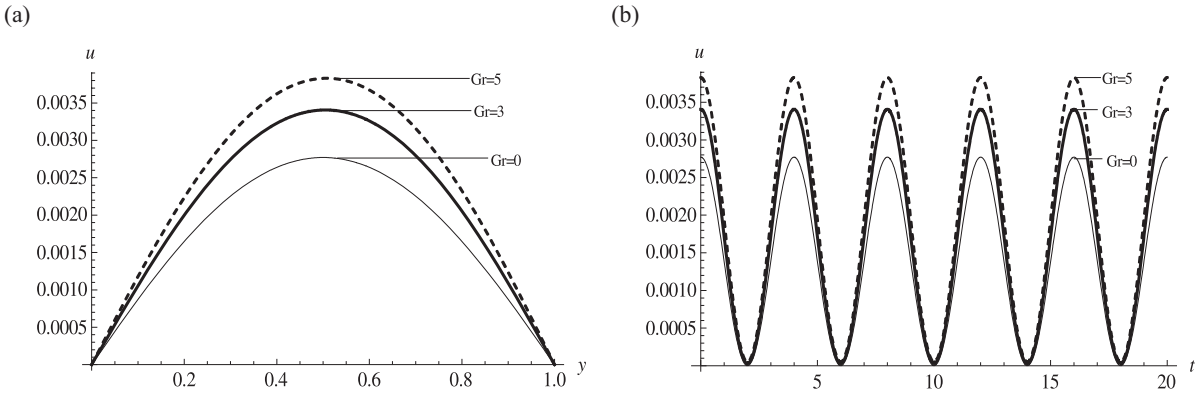

Fig. 4. (a) Velocity distribution plotted against position; (b) velocity distribution plotted against time.

subject to the following boundary conditions:

$$A(0)=0,\ \ A(1)=1, \tag{20}$$
$$B(0)=0,\ \ B(1)=1, \tag{21}$$
$$v(0)=0=v''(0),\ \ v(1)=0=v''(1), \tag{22}$$
$$w(0)=0=w''(0),\ \ w(1)=0=w''(1). \tag{23}$$

Using the solutions of (16) and (17) with the boundary conditions (20)–(21), respectively, we write the exact solution of (15) as

$$\begin{aligned}\theta(t,y) &= m_1\left(\mathrm{e}^{m_2 y}-\mathrm{e}^{m_3 y}\right)\\ &\quad + m_4\left(\mathrm{e}^{m_5 y}-\mathrm{e}^{m_6 y}\right)\mathrm{e}^{\mathrm{i}\omega t},\end{aligned} \tag{24}$$

where the constants $m_i's$ are defined in the Appendix.

A direct integration of (18) and (19) subject to the boundary conditions at $y=0$ in (22)–(23) gives the integral equations

$$\begin{aligned}v(y) &= \int_0^y a_1\,\mathrm{d}y+\int_0^y\int_0^y\int_0^y a_2\,\mathrm{d}y\,\mathrm{d}y\,\mathrm{d}y\\ &\quad+\int_0^y\int_0^y\int_0^y\int_0^y a^2\left[\mathrm{Re}p_1+\mathrm{Re}\,\mathrm{Gr}A(y)\right.\\ &\quad\left.-\mathrm{Re}\frac{\mathrm{d}v}{\mathrm{d}y}+\beta\frac{\mathrm{d}^2v}{\mathrm{d}y^2}-H^2v\right]\mathrm{d}y\,\mathrm{d}y\,\mathrm{d}y\,\mathrm{d}y\end{aligned} \tag{25}$$

and

$$\begin{aligned}w(y) &= \int_0^y b_1\,\mathrm{d}y+\int_0^y\int_0^y\int_0^y b_2\,\mathrm{d}y\,\mathrm{d}y\,\mathrm{d}y\\ &\quad+\int_0^y\int_0^y\int_0^y\int_0^y a^2\left(\mathrm{Re}p_0\right.\\ &\quad+\mathrm{Re}\,\mathrm{Gr}B(y)-\mathrm{Re}\frac{\mathrm{d}w}{\mathrm{d}y}+\beta\frac{\mathrm{d}^2w}{\mathrm{d}y^2}\\ &\quad\left.-(H^2+\mathrm{i}\mathrm{Re}\omega)w\right)\mathrm{d}y\,\mathrm{d}y\,\mathrm{d}y\,\mathrm{d}y,\end{aligned} \tag{26}$$

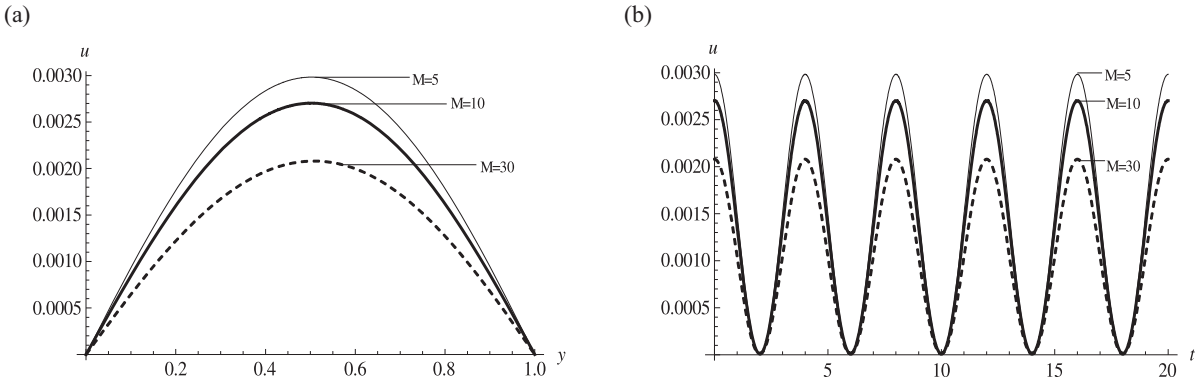

Fig. 5. (a) Velocity distribution plotted against position; (b) velocity distribution plotted against time.

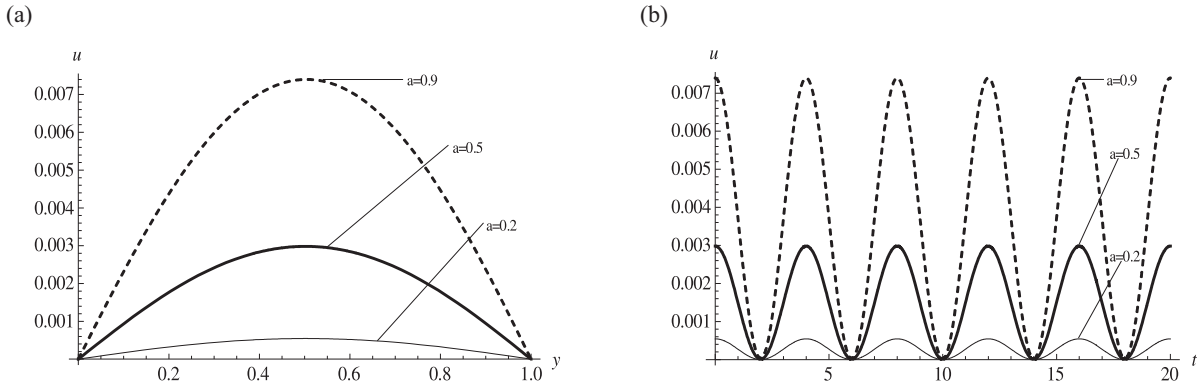

Fig. 6. (a) Velocity distribution plotted against position; (b) velocity distribution plotted against time.

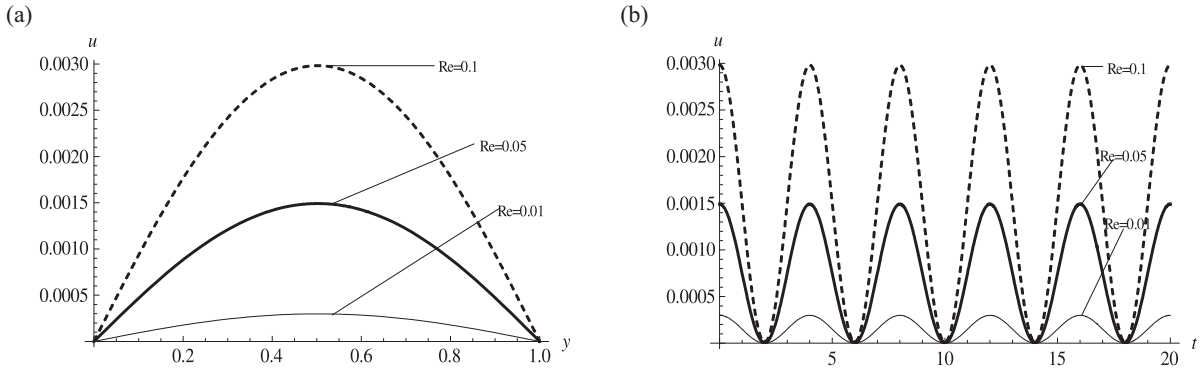

Fig. 7. (a) Velocity distribution plotted against position; (b) velocity distribution plotted against time.

respectively, where

$$a_1 = \frac{\mathrm{d}v(0)}{\mathrm{d}y}, \quad b_1 = \frac{\mathrm{d}w(0)}{\mathrm{d}y},$$
$$a_2 = \frac{\mathrm{d}^3v(0)}{\mathrm{d}y^3}, \quad b_2 = \frac{\mathrm{d}^3w(0)}{\mathrm{d}y^3}.$$

To obtain the solution of the integral equations using the Adomian decomposition approach [16]–[25], we seek a series solution in the form

$$v = \sum_{n=0}^{\infty} v_n(y), \tag{27}$$

$$w = \sum_{n=0}^{\infty} w_n(y). \tag{28}$$

Substituting (27) and (28) in (25)–(26) leads to the recursive relations

$$v_0(y) = ya_1 + \frac{y^3}{6}a_2 + \frac{a^2P_1\mathrm{Re}}{24}y^4 + \int_0^y\int_0^y\int_0^y\int_0^y a^2\mathrm{Re}\,\mathrm{Gr}A(y)\,\mathrm{d}y\,\mathrm{d}y\,\mathrm{d}y\,\mathrm{d}y,$$
$$v_{n+1}(y) = \int_0^y\int_0^y\int_0^y\int_0^y a^2\left(-\mathrm{Re}\frac{\mathrm{d}v_n}{\mathrm{d}y} + \beta\frac{\mathrm{d}^2v_n}{\mathrm{d}y^2} - Hv_n\right)\mathrm{d}y\,\mathrm{d}y\,\mathrm{d}y\,\mathrm{d}y \tag{29}$$

and

$$w_0 = yb_1 + \frac{y^3}{6}b_2 + \frac{a^2}{24}\mathrm{Re}p_0y^4 + \int_0^y\int_0^y\int_0^y\int_0^y a^2\mathrm{Re}\,\mathrm{Gr}B(y)\,\mathrm{d}y\,\mathrm{d}y\,\mathrm{d}y\,\mathrm{d}y,$$
$$w_{n+1} = \int_0^y\int_0^y\int_0^y\int_0^y a^2\left(-\mathrm{Re}\frac{\mathrm{d}w_n}{\mathrm{d}y} + \beta\frac{\mathrm{d}^2w_n}{\mathrm{d}y^2} - (H^2 + \mathrm{iRe}\omega)w_n\right)\mathrm{d}y\,\mathrm{d}y\,\mathrm{d}y\,\mathrm{d}y. \tag{30}$$

Using mathematica software, few terms of the recursive relations (29)–(30) are obtained, and the con-

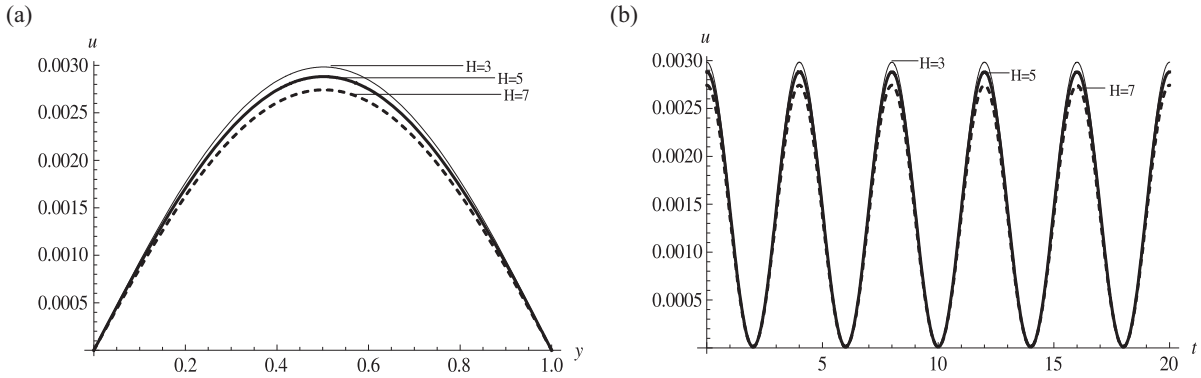

Fig. 8. (a) Velocity distribution plotted against position; (b) velocity distribution plotted against time.

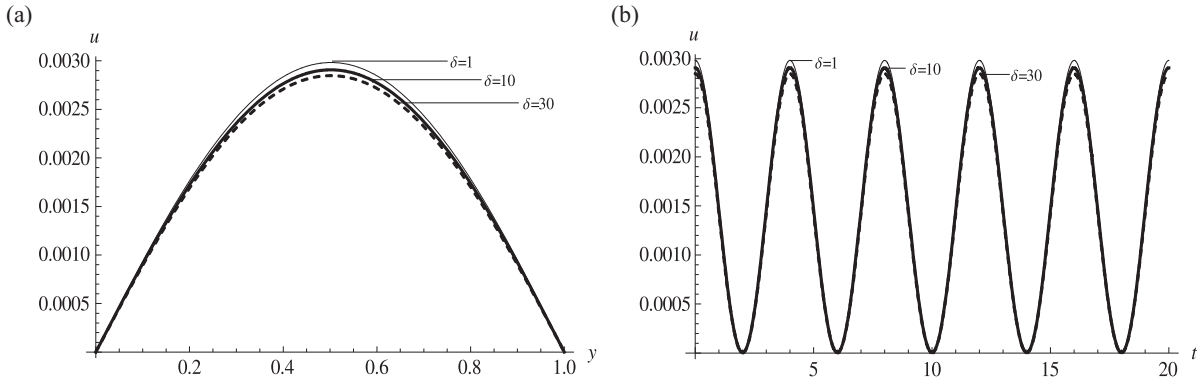

Fig. 9. (a) Velocity distribution plotted against position; (b) velocity distribution plotted against time.

stants a_1, a_2 and b_1, b_2 are determined using the boundary conditions at $y = 1$ in (22) – (23), respectively. Then the partial sums

$$v = \sum_{n=0}^{h} v_n(y)\,, \tag{31}$$

$$w = \sum_{n=0}^{h} w_n(y) \tag{32}$$

of the series solution (27) – (28) are substituted in (14) as the analytical solution of the problem.

The shear stress at the upper wall of the channel is given by

$$\tau = -(1+M)\left.\frac{\partial u}{\partial y}\right|_{y=1}. \tag{33}$$

In addition, the rate of heat transfer across the channel is given by

$$\begin{aligned} \mathrm{Nu} = \frac{\partial \theta}{\partial y} &= m_1\left(m_2\,\mathrm{e}^{m_2 y} - m_3\,\mathrm{e}^{m_3 y}\right) \\ &+ m_4\left(m_5\,\mathrm{e}^{m_5 y} - m_6\,\mathrm{e}^{m_6 y}\right)\mathrm{e}^{\mathrm{i}\omega t}\,, \end{aligned} \tag{34}$$

where Nu is the Nusselt number.

4. Discussion of Results

It is imperative to mention from the beginning that the definition of the radiative heat flux given in (5) may be interpreted as heat absorbing whenever $T_0 > T$ and heat-emitting if $T_0 < T$. However in this paper, the heat-emitting case is considered and results are discussed accordingly. In addition, the real parts of the solutions are considered. Therefore, in the present study the unsteady flow of a viscous incompressible and electrically conducting non-Newtonian fluid through porous parallel plates with non-uniform wall temperature is studied, results are computed for various val-

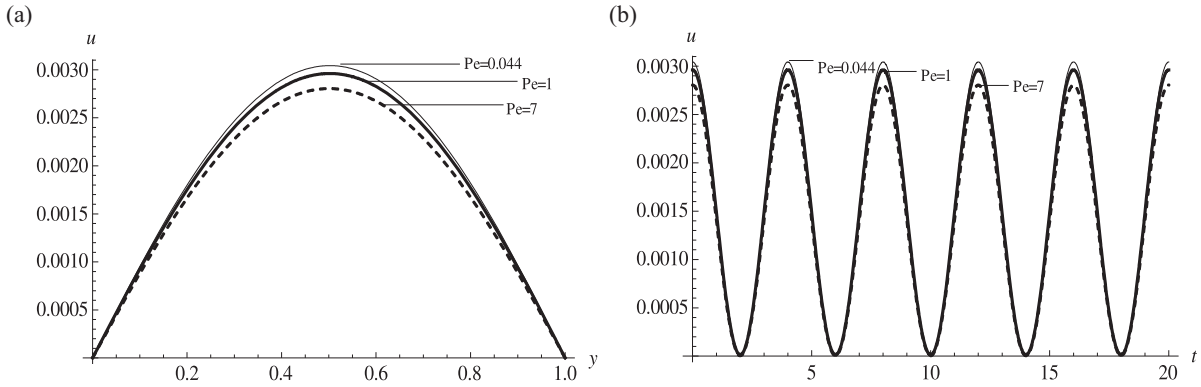

Fig. 10. (a) Velocity distribution plotted against position; (b) velocity distribution plotted against time.

ues of the flow parameters and are presented graphically in Figures 2–14 for fixed values of $\omega = \pi$, $P_0 = P_1 = 5$.

In Figure 2, the effect of the Peclet number on the temperature distribution is presented for $t = 0$ and $y = 0.5$, respectively, for $\delta = 0.1$, and the result shows that an increase in Peclet number decreases the temperature within the channel; this is due to a decrease in thermal diffusivity. Figure 3 represents the effect of radiation on the temperature profile for $t = 0$ and $y = 0.5$, respectively, when Pe $= 0.71$. From the graph, it is observed that the temperature is lower at the cold wall with injection and higher at the heated wall where the fluid is sucked and increases in an exponential manner satisfying the boundary conditions. It is observed further that an increase in the thermal radiation parameter decreases the temperature distribution within the channel by decreasing the thermal boundary layer thickness. Figure 4 shows the effect of the thermal buoyancy force parameter on the hydromagnetic non-Newtonian couple stress fluid flow for $t = 0$ and $y = 0.5$, respectively, when Pe $= 0.71$, $H = 3$, $M = 5$, Re $= 0.1$, $\delta = 1$, and $a = 0.5$. As observed from the graph, the maximum flow occurs at the maximum Gr $= 5$ and minimum at Gr $= 0$ which corresponds to the hydrodynamic case studied in [1]. This shows that the buoyancy force has a significant influence on the flow.

The effect of an increase in the non-Newtonian parameter on the fluid flow is represented in Figure 5 for $t = 0$ and $y = 0.5$, respectively, when $a = 0.5$, Pe $= 0.71$, $H = 3$, Gr $= 1$, Re $= 0.1$, and $\delta = 1$. As seen from the graph, the increase in the non-Newtonian parameter decreases the velocity maximum. It is interesting to note that the effect of the non-Newtonian parameter is prominent in the core region of the channel and has minima at the boundaries; this is due to an

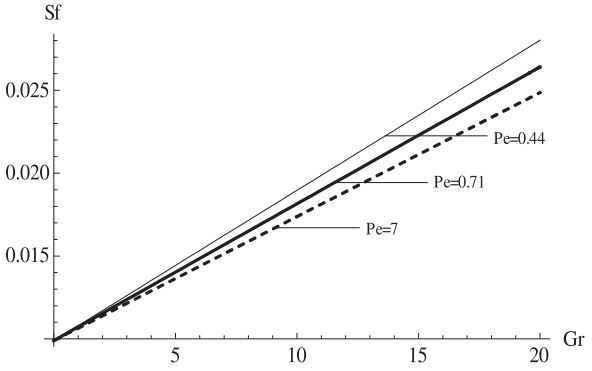

Fig. 11. Variations in skin friction for $t = 0$ and $y = 1$, respectively, when $M = H = 1$, $a = 0.5$, Re $= 0.1$, $\delta = 1$.

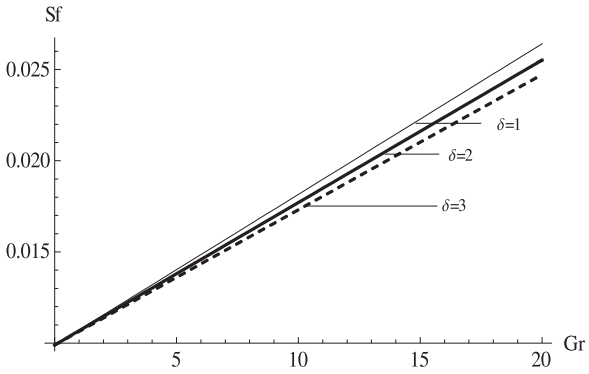

Fig. 12. Variations in skin friction with Grashof number for $t = 0$ and $y = 1$, respectively, when $M = H = 1$, $a = 0.5$, Re $= 0.1$, Pe $= 0.71$.

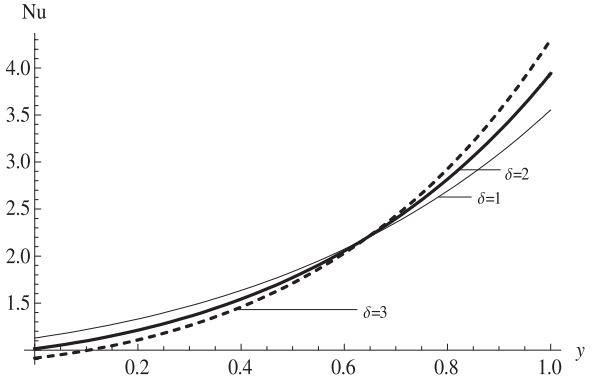

Fig. 13. Variations in Nusselt number with radiation parameter.

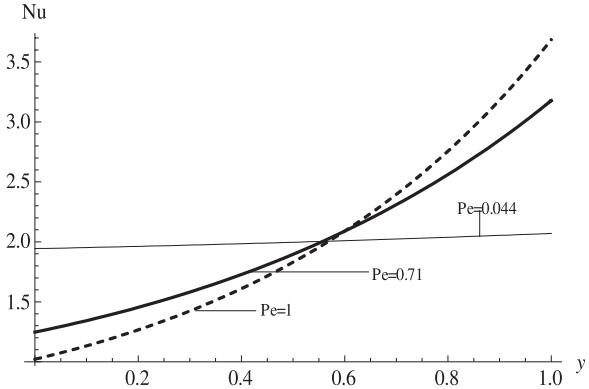

Fig. 14. Variations in Nusselt number with Peclet number.

increase in the frictional force within the fluid layers. Figure 6 represents the influence of the couple stress inverse a^2 on the flow for $t = 0$ and $y = 0.5$, respectively, when Pe $= 0.71$, $H = 3$, Gr $= 1$, Re $= 0.1$, $\delta = 1$, and $M = 5$. It is observed that the increase in the couple stress inverse enhances the flow velocity. Ultimately, the effect of couple stresses on the flow decreases the flow maximum; this result is in perfect agreement with previous results in literature. It is observed in Figure 7 that an increase in the Reynolds number improves the flow velocity for $t = 0$ and $y = 0.5$, respectively, when Pe $= 0.71$, $H = 3$, Gr $= 1$, $\delta = 1$, and $M = 5$. This is so due to the fact that the viscous force in the non-Newtonian fluid dominates over the inertia force, that account for the reason why the velocity has a minimum at the point where the inertia force has a minimum and the velocity is maximum where the inertia force is maximum. If the inertia force continue to grow then the disturbances within the fluid will lead to a break down in the laminar flow.

In Figure 8, the effect of an imposed magnetic field placed transversely to the channel is presented for $t = 0$ and $y = 0.5$, respectively, when $a = 0.5$, Pe $= 0.71$, $M = 5$, Gr $= 1$, Re $= 0.1$, and $\delta = 1$. As seen from the two plots a and b, the maximum flow occurs when the magnetic field is at its minimum value, therefore increase in the Hartmann number decreases the flow; this is due to the retarding effect of the Lorentz force when placed normal to the flow channel. The effect of this retarding force is observed as the Hartmann number increases. It is important to note that this finds its application in the control of hot fluid flow during metal processing.

A velocity profile is plotted for different values of the thermal radiation parameter in Figure 9 for $t = 0$ and $y = 0.5$, respectively, when $a = 0.5$, Pe $= 0.71$, $H = 3$, Gr $= 1$, Re $= 0.1$, and $M = 5$. It is observed that the velocity maximum increases with a decrease in the radiation parameter, especially in the centre of the channel, and decreases with an increase in the Peclet number as observed from Figure 10 for $t = 0$ and $y = 0.5$, respectively, when $M = 5$, $a = 0.5$, $H = 3$, Gr $= 1$, Re $= 0.1$, and $\delta = 1$.

Figures 11 – 12 represent the effect of thermal radiation and Peclet number on the skin friction on the heated wall; it is observed that the skin friction increases with an increase in Grashof number while both Peclet number and radiation parameter decrease the magnitude of skin friction. Figures 13 – 14 show the rate of heat transfer within the channel for variations in radiation parameter and Peclet number, respectively. As observed from the figures, both parameters increase the heat being transferred from the heated wall to the fluid; also at the cold wall, heat is transferred from the fluid to the plate.

5. Conclusion

In the present work, an analytical approach to investigate the influence of temperature on the hydromagnetic flow of a non-Newtonian couple stress fluid through a porous channel is presented in the form of Adomian decomposition method and by taking into account the radiative heat flux in the optically thin limit. There is perfect agreement between the present work and the hydrodynamic case investigated

by [1] when Gr = 0. In the present work, we conclude that increasing Peclet number and radiation parameter have decreasing effects on both temperature and velocity profile while increase in Grashof number leads to an increase in the flow velocity; finally, increasing the radiative heat flux parameter decreases both the temperature and the velocity profile in the channel. Additionally, the results show that an increase in both Peclet number and radiation parameter reduces the skin friction on the heated wall while the Grashof number increases the skin friction on the heated wall.

Acknowledgements

S. O. A. is full of thanks to the anonymous reviewers for their helpful comments in improving this paper.

Appendix

$$m_1 = -\frac{\exp\left[\frac{1}{2}\left(-\mathrm{Pe}+\sqrt{\mathrm{Pe}}\sqrt{\mathrm{Pe}+4\delta}\right)\right]}{-1+\exp\left[\sqrt{\mathrm{Pe}}\sqrt{\mathrm{Pe}+4\delta}\right]},$$

$$m_2 = \frac{1}{2}\left(\mathrm{Pe}-\sqrt{\mathrm{Pe}}\sqrt{\mathrm{Pe}+4\delta}\right),$$

$$m_3 = \frac{1}{2}\left(\mathrm{Pe}+\sqrt{\mathrm{Pe}}\sqrt{\mathrm{Pe}+4\delta}\right),$$

$$m_4 = -\frac{\exp\left[\frac{1}{2}\left(-\mathrm{Pe}+\sqrt{\mathrm{Pe}}\sqrt{\mathrm{Pe}+4\mathrm{i}\omega+4\delta}\right)\right]}{-1+\exp\left[\sqrt{\mathrm{Pe}}\sqrt{\mathrm{Pe}+4\mathrm{i}\omega+4\delta}\right]},$$

$$m_5 = \frac{1}{2}\left(\mathrm{Pe}-\sqrt{\mathrm{Pe}}\sqrt{\mathrm{Pe}+4\mathrm{i}\omega+4\delta}\right),$$

$$m_6 = \frac{1}{2}\left(\mathrm{Pe}+\sqrt{\mathrm{Pe}}\sqrt{\mathrm{Pe}+4\mathrm{i}\omega+4\delta}\right).$$

[1] N. T. M. Eldabe, A. A. Hassan, and M. A. A. Mohamed, Z. Naturforsch. **58a**, 204 (2003).
[2] J. Zueco and O. A. Bég, Int. J. Appl. Math. Mech. **5**, 1 (2009).
[3] S. O. Adesanya and R. O. Ayeni, Int. J. Nonlin. Sci. **12**, 6 (2011).
[4] M. Zakaria, Appl. Math. Comput. **139**, 265 (2003).
[5] O. D. Makinde and P. Y. Mhone, Rom. J. Phys. **50**, 931 (2005).
[6] A. Mahmoud and A. Ali, Rom. J. Phys. **52**, 85 (2007).
[7] A. K. A. Hakeem and K. Sathiyanathan, Nonlin. Anal. **3**, 288 (2009).
[8] C.-C. Tsai and T.-W. Hsu, Comput. Fluids **39**, 696 (2010).
[9] B. K. Jha and A. O. Ajibade, Int. Commun. Heat Mass Trans. **36**, 624 (2009).
[10] C.-W. Chang-Jian, H.-T. Yau, and J.-L. Chen, Appl. Math. Model. **34**, 2493 (2010).
[11] C.-W. Chang-Jian and C.-K. Chen, Appl. Math. Model. **34**, 1763 (2010).
[12] D. Srinivasacharya and D. Srikanth, C. R. Mecanique **336**, 820 (2008).
[13] K. S. Mekheimer and Y. Abd elmaboud, Physica A **387**, 2403 (2008).
[14] A. Ali and A. Mahmoud, J. Appl. Math. Anal. Appl. **1**, 125 (2005).
[15] A. Mahmoud, A. Ali, and T. Mahmoud, Punjab Uni. J. Math. **41**, 35 (2009).
[16] G. Adomian, Solving Frontier Problem in Physics, Kluwer Publication Boston, Boston 1994.
[17] V. Daftardar-Gejji and H. Jafari, Appl. Math. Comput. **189**, 541 (2007).
[18] A. M. Wazwaz, Appl. Math. Comput. **166**, 638 (2005).
[19] K. Haldar, Appl. Math. Lett. **9**, 109 (1996).
[20] B. Zhang, Q.-B. Wu, and X.-G. Luo, Appl. Math. Comput. **175**, 1495 (2006).
[21] A. M. Wazwaz, Appl. Math. Comput. **182**, 1812 (2006).
[22] H. Haddadpour, Math. Comput. Model. **44**, 1144 (2006).
[23] S. Nadeem and N. S. Akbar, Commun. Nonlin. Sci. Numer. Simul. **14**, 3844 (2009).
[24] M. Tataria, M. Dehghana, and M. Razzaghi, Math. Comput. Model. **45**, 639 (2007).
[25] S. O. Adesanya and R. O. Ayeni, Int. e. J. Pure Appl. Math., (Accepted Manuscript).